Odd parity bottom-flavored baryon resonances

C. García-Recio[1], J. Nieves[2], O. Romanets[3], L. L. Salcedo[1], L. Tolos[4,5]

[1]*Departamento de Física Atómica, Molecular y Nuclear,*
and Instituto Carlos I de Física Teórica y Computacional,
Universidad de Granada, E-18071 Granada, Spain
[2]*Instituto de Física Corpuscular (centro mixto CSIC-UV),*
Institutos de Investigación de Paterna,
Aptdo. 22085, 46071, Valencia, Spain
[3]*KVI, University of Groningen, Zernikelaan 25,*
9747AA Groningen, The Netherlands
[4]*Institut de Ciències de l'Espai (IEEC/CSIC),*
Campus Universitat Autònoma de Barcelona,
Facultat de Ciències, Torre C5,
E-08193 Bellaterra, Spain
[5]*Frankfurt Institute for Advanced Studies,*
Johann Wolfgang Goethe University,
Ruth-Moufang-Str. 1, 60438 Frankfurt am Main
(Dated: February 6, 2013)

The LHCb Collaboration has recently observed two narrow baryon resonances with beauty. Their masses and decay modes look consistent with the quark model orbitally excited states $\Lambda_b(5912)$ and $\Lambda_b^*(5920)$, with quantum numbers $J^P = 1/2^-$ and $3/2^-$, respectively. We predict the existence of these states within a unitarized meson-baryon coupled-channel dynamical model, which implements heavy-quark spin symmetry. Masses, quantum numbers and couplings of these resonances to the different meson-baryon channels are obtained. We find that the resonances $\Lambda_b^0(5912)$ and $\Lambda_b^0(5920)$ are heavy-quark spin symmetry partners, which naturally explains their approximate mass degeneracy. Corresponding bottom-strange baryon resonances are predicted at $\Xi_b(6035.4)$ ($J^P = \frac{1}{2}^-$) and $\Xi_b(6043.3)$ ($J^P = \frac{3}{2}^-$). The two Λ_b and two Ξ_b resonances complete a multiplet of the combined symmetry SU(3)-flavor times heavy-quark spin.

I. INTRODUCTION

Using pp collision data at $7\,\mathrm{TeV}$ center of mass energy, the LHCb Collaboration [1] has reported the existence of two narrow states observed in the $\Lambda_b^0 \pi^+ \pi^-$ spectrum, with masses $5911.95 \pm 0.12\,(stat) \pm 0.03\,(syst) \pm 0.66\,(\Lambda_b^0\,\mathrm{mass})\,\mathrm{MeV}$, and $5919.76 \pm 0.07\,(stat) \pm 0.02\,(syst) \pm 0.66\,(\Lambda_b^0\,\mathrm{mass})\,\mathrm{MeV}$. These states are interpreted as the orbitally-excited $\Lambda_b^0(5912)$ and $\Lambda_b^0(5920)$ bottom baryon resonances, with spin–parity $J^P = 1/2^-$ and $J^P = 3/2^-$, respectively. The limits on the natural widths of these states are $\Gamma_{\Lambda_b^0(5912)} \leq 0.82\,\mathrm{MeV}$ and $\Gamma_{\Lambda_b^0(5920)} \leq 0.72\,\mathrm{MeV}$ at the 95% confidence level [1].

There exists an old prediction by Capstick and Isgur for the masses of these two Λ_b resonances which is in very good agreement with the results reported by the LHCb collaboration. Indeed, their relativistic quark model predicts $5912\,\mathrm{MeV}$ and $5920\,\mathrm{MeV}$ for the masses of the lightest orbitally-excited states [2]. However, the same model yields a mass of the ground state Λ_b^0 ($J^P = 1/2^+$) which is about $35\,\mathrm{MeV}$ smaller than the measured value [3]. More recently, Garcilazo et al. [4] have also presented results from a constituent quark model scheme. They adjusted the mass of the Λ_b^0 ground state and predicted the masses of the $J^P = 1/2^-$ and $3/2^-$ orbitally excited Λ_b states, which turned out to be around $30\,\mathrm{MeV}$ lower than the LHCb experimen-

tal values. Note however that the masses predicted in [4] are in turn 20-30 MeV higher than those obtained in other schemes based also on the relativistic quark model [5], or on the color hyperfine interaction [6] or on the heavy quark effective theory [7]. More recently, in [8] heavy baryonic resonances Λ_b (Λ_c) with $J^P = 3/2^-$ are studied in a constituent quark model as a molecular state composed by nucleons and $\bar{B}^*$ (D^*) mesons.

In this work we adopt a different approach and describe these odd parity excited states as dynamically generated resonances obtained within a unitarized meson-baryon coupled-channel scheme. It is known that some baryon states can be constructed as a qqq state in a quark model, and simultaneously as a dynamically generated resonance in a meson-baryon coupled-channel description (that is a $qqq - q\bar{q}$ molecular state) [9]. Though, some of their properties might differ. It is thus interesting to consider both points of view in order to get in the future a joint or integral description of hadronic resonances in terms of quarks and hadrons degrees of freedom.

The unitarization in coupled-channels has proven to be very successful in describing some of the existing experimental data. Such studies include approaches based on the chiral perturbation theory amplitudes for scattering of 0^- octet Goldstone bosons off baryons of the $1/2^+$ nucleon octet in the charmless sector [10–29]. Unitarized coupled-channel methods have been further ex-

tended to the baryon-meson sector with charm degrees of freedom under several variants: The works in [30–38] use a bare baryon-meson interaction saturated with the t-channel exchange of vector mesons between pseudoscalar mesons and baryons. The works in [39–41] are based on the Jülich meson-exchange model. Those in [42–44] apply the hidden gauge formalism, and the same approach has been extended to the bottom sector in [45]. Finally, an extended Weinberg-Tomozawa (WT) interaction is used in [46–48].

Of special importance are the symmetries that are implemented in the quark or hadronic models. Typically, while hadronic models pay an special attention to chiral symmetry, quark models usually implement heavy-quark spin symmetry (HQSS). HQSS is a direct consequence of QCD [49–51]. It states that the interaction dependent on the spin state of the heavy quark is of $O(\Lambda_{\rm QCD}/m_Q)$, and so suppressed in the infinite quark mass limit. For instance, the vector and pseudoscalar mesons with a bottom quark, which only differ in how the spins of light and heavy quarks are coupled, form a doublet of HQSS and would be degenerate in the infinite mass limit. So, HQSS requires the pseudoscalar $\bar{B}$ ($\bar{B}_s$) meson and the $\bar{B}^*$ ($\bar{B}_s^*$) meson, its vector partner, to be treated on an equal footing. On the other hand, chiral symmetry fixes the lowest order interaction between Goldstone bosons and other hadrons in a model independent way; this is the WT interaction. Thus, it is appealing to have a predictive model for four flavors including all basic hadrons (pseudoscalar and vector mesons, and $\frac{1}{2}^+$ and $\frac{3}{2}^+$ baryons) which reduces to the WT interaction in the sector where Goldstone bosons are involved and which incorporates HQSS in the sector where bottom quarks participate.

In this letter we use hadronic degrees of freedom in a unitarized meson-baryon coupled-channel calculation. We rely on a tree-level contact interaction that embodies the approximate pattern of both chiral symmetry, when Goldstone bosons are involved, and HQSS when heavy hadrons are present. Moreover, it enjoys spin-flavor symmetry in the light (u, d, s) flavor sector. The scheme has been successfully used for describing odd parity s-wave light flavor [52] and charm [46–48] baryon resonances. Indeed, the model naturally explains the overall features (masses, widths and main couplings) of the corresponding resonances ($\Lambda_c^+(2595)$ and $\Lambda_c^+(2625)$) that appear in the charm sector ($C = 1$) [46, 47]. Further predictions of this model for the $C = -1$ sector can be found in [48, 53].

HQSS is not explicitly accounted for in other unitarized coupled-channel models [30–45], as they typically give an asymmetric treatment to heavy mesons that are HQSS partners. Nevertheless, a detailed analysis of the hidden gauge model as applied in [42, 43, 45] shows no actual violation in the heavy quark limit [54].[1]

The paper is organized as follows. In Sec. II we present the features of our coupled-channel unitarized approach while in Sec. III we show the results not only for (Λ_b, Λ_b^*) but also for (Ξ_b, Ξ_b^*) states, which belong to the same SU(3)×HQSS multiplets. Finally, we present our conclusions in Sec. IV.

II. COUPLED-CHANNELS AND UNITARIZATION

We follow here the approach already applied in Refs. [46–48] for charm quarks. We will consider a system with baryon number one, one bottom quark ($B = -1$) and strangeness, isospin and spin-parity given by: $(S, I, J^P) = (0, 0, 1/2^-)$ denoted as Λ_b, $(0, 0, 3/2^-)$ as Λ_b^*, $(-1, 1/2, 1/2^-)$ as Ξ_b and $(-1, 1/2, 3/2^-)$ as Ξ_b^*.

All meson-baryon pairs with the same SIJ quantum numbers span the coupled-channel space. We apply s-wave amplitudes. This seems appropriate in our case since the observed resonances are close to threshold. The tree-level contact amplitudes between two channels ij for each SIJ sector are given by:

$$V_{ij}^{SIJ} = D_{ij}^{SIJ} \frac{2\sqrt{s} - M_i - M_j}{4 f_i f_j} \sqrt{\frac{E_i + M_i}{2M_i}} \sqrt{\frac{E_j + M_j}{2M_j}},$$
(1)

where $\sqrt{s}$ is the center of mass (C.M.) energy of the system; E_i and M_i are, respectively, the C.M. energy and mass of the baryon in the channel i; and f_i is the decay constant of the meson in the i-channel. The masses of baryons with bottom content used in this work are compiled in Table I, while those of the bottom mesons and their decay constants are given in Table II. The rest of hadron masses and meson decay constants not shown in the above tables have been taken from Ref. [47].

Finally the coefficients D_{ij}^{SIJ} come from the underlying spin-flavor extended WT structure of the couplings in our model [46, 47, 55]. Tables for the coefficients can be found in the Appendices B of Refs. [46, 47]. The coefficients to be used for the $B = -1$ sector (one bottom quark interacting with light quarks) are identical to those for $C = 1$ (one charm quark interacting with light quarks) with obvious renaming of the heavy hadrons. The universality of the interactions of heavy quarks, regardless of their concrete (large) mass, flavor and spin state, follows from QCD [49–51] and it is automatically implemented in our model. Let us note that such emerging heavy spin-flavor symmetry, which becomes exact in the infinitely heavy quark limit, is different from the approximate SU(6) or light spin-flavor symmetry, also implemented in our model.

---

[1] The would-be offending amplitudes are either not actually in-

cluded due to the large gap between channels (e.g., $\Lambda_b B \to N\pi$) or they would be suppressed in the heavy quark limit due to the presence of a heavy vector-meson exchange propagator (e.g., $\Lambda_c \bar{D} \to N\eta_c$).

We remark that the various exact symmetries referred to above (chiral, spin-flavor and HQSS) apply only to the coefficients D_{ij}^{SIJ}, while physical masses and decay meson constants are used throughout when solving the coupled-channel equations. The symmetry content of our model can be exposed by artificially changing these hadron properties (masses and decay constants) to enforce spin-flavor, flavor and/or heavy quark spin symmetries. If, starting from the physical values, $SU(3) \times HQSS$ is adiabatically enforced, the resonances so obtained organize themselves into exact $SU(3) \times HQSS$ multiplets. In this way this approximate symmetry can be used to label the physical states. The largest exact symmetry present in the coefficients D_{ij}^{SIJ} is $SU(6) \times HQSS$, so the physical states can also be classified under approximate multiplets of this symmetry.[2] We apply such group label assignments to our results.

We use the matrix V^{SIJ} as kernel to solve the Bethe-Salpeter equation, which provides the T-matrix as

$$T^{SIJ} = (1 - V^{SIJ}G^{SIJ})^{-1}V^{SIJ}. \qquad (2)$$

Here G^{SIJ} is a diagonal matrix containing the two particle propagator for each channel. Explicitly

$$G_{ii}^{SIJ} = 2M_i \left(\bar{J}_0(\sqrt{s}; M_i, m_i) - \bar{J}_0(\mu^{SI}; M_i, m_i) \right), \qquad (3)$$

where m_i is the mass of the meson in the channel i. The loop function $\bar{J}_0$ can be found in the Appendix of Ref. [17] for the different relevant Riemann sheets. The two particle propagator diverges logarithmically. The loop is renormalized by a subtraction constant such that

$$G_{ii}^{SIJ} = 0 \quad \text{at} \quad \sqrt{s} = \mu^{SI}. \qquad (4)$$

To fix the subtraction point μ^{SI}, we apply the following prescription: μ^{SI} equals $\sqrt{m_{\text{th}}^2 + M_{\text{th}}^2}$, where m_{th} and M_{th} are, respectively, the masses of the meson and the baryon of the channel with the lowest threshold (minimal value of $m_{\text{th}} + M_{\text{th}}$) among all the channels with the given values of S and I and any value of J. Therefore the subtraction point takes a common value for all sectors SIJ with equal SI. This renormalization scheme (RS) was first proposed in [33, 34]. Successful results from this RS, but involving only the mesons and baryons of the pion and nucleon octets were already obtained in [25]. This specific RS is just a prescription which previously has produced good results, but it can be refined when phenomenological information is available.[3] We will study this possibility in the next section.

The dynamically-generated baryon resonances can be obtained as poles of the scattering amplitudes in each of

Baryon	$M\,[\text{MeV}]$	$\Gamma\,[\text{MeV}]$	SU(6)	SU(3)$_{2J+1}$	HQSS
Λ_b	5619.37 [56]		**21**	$\mathbf{3_2^*}$	singlet
Ξ_b	5789.55 [3]		**21**	$\mathbf{3_2^*}$	singlet
Σ_b	5813.4 [3]	7.3	**21**	$\mathbf{6_2}$	doublet
Σ_b^*	5833.55 [3]	9.5	**21**	$\mathbf{6_4}$	doublet
Ξ_b'	5926 [58]		**21**	$\mathbf{6_2}$	doublet
Ξ_b^*	5945 [63]		**21**	$\mathbf{6_4}$	doublet
Ω_b	6050.3 [64]		**21**	$\mathbf{6_2}$	doublet
Ω_b^*	6069 [65]		**21**	$\mathbf{6_4}$	doublet

TABLE I: Baryon masses and widths used throughout this work. The SU(6) and SU(3)$_{2J+1}$ labels are also displayed. The last column indicates the HQSS multiplets. Members of a HQSS doublet are placed in consecutive rows.

Meson	$m\,[\text{MeV}]$	$f\,[\text{MeV}]$	SU(6)	SU(3)$_{2J+1}$	HQSS
$\bar{B}$	5279.335 [3]	133.6 [66]	$\mathbf{6^*}$	$\mathbf{3_1^*}$	doublet
$\bar{B}^*$	5325.2 [3]	$f_{\bar{B}}$	$\mathbf{6^*}$	$\mathbf{3_3^*}$	doublet
$\bar{B}_s$	5366.3 [3]	159.1 [67]	$\mathbf{6^*}$	$\mathbf{3_1^*}$	doublet
$\bar{B}_s^*$	5415.4 [3]	$f_{\bar{B}_s}$	$\mathbf{6^*}$	$\mathbf{3_3^*}$	doublet

TABLE II: Meson masses, m, and decay constants, f, used throughout this work. The SU(6) and SU(3)$_{2J+1}$ labels are also displayed. The last column indicates the HQSS multiplets. Members of a HQSS doublet are placed in consecutive rows.

the SIJ sectors. We look at both the first and second Riemann sheets of the variable $\sqrt{s}$. The poles of the scattering amplitude on the first Riemann sheet that appear on the real axis below threshold are interpreted as bound states. The poles that are found on the second Riemann sheet below the real axis and above threshold are identified with resonances.[4] The mass and the width of the bound state/resonance can be found from the position of the pole on the complex energy plane. Close to the pole, the T-matrix behaves as

$$T_{ij}^{SIJ}(s) \approx \frac{g_i e^{i\phi_i} \, g_j e^{i\phi_j}}{\sqrt{s} - \sqrt{s_R}} . \qquad (5)$$

$\sqrt{s_R} = M_R - i\Gamma_R/2$ provides the mass (M_R) and the width (Γ_R) of the resonance, and $g_j e^{i\phi_j}$ (modulus and phase) is the coupling of the resonance to the channel j.

There is a technical aspect which should be addressed at this point. It follows from QCD that, as one flavor of quarks becomes heavy, the spectrum of hadrons with one such quark tends to a universal pattern, shifted by the heavy quark mass. However, it is well known [17]

---

[2] The requirement of SU(6) × HQSS still allows many possible interactions so spin-flavor SU(8) is used to reduce the number of parameters, but this symmetry is explictly broken, even at the level of coefficients, in order to have exact HQSS [47].

[3] See [29] for a discussion on the subtraction point and its natural vs. phenomenological values.

[4] Often we refer to all poles generically as resonances, regardless of their concrete nature, since usually they can decay through other channels not included in the model space.

that the renormalized loop function, G, grows logarithmically as any one of the hadrons in the loop gets heavy. This implies that, in the infinitely heavy quark limit, the interaction (and so the binding energy in attractive sectors) would effectively increase at a logarithmic rate, rather than stabilizing. By artificially increasing the bottomed hadron masses we have verified that such spurious binding would indeed arise for sufficiently large masses,[5] however, it is not clear how sizable the effect is in a realistic scenario. As will be seen below, the generic subtraction point defined after Eq. (4) actually produces too little binding and we have to move to a phenomenological subtraction point to pinpoint the experimentally observed states. This would suggest that the problem is not yet a pressing one at the bottom scale, at least for the sector we are considering and those related to it by softly broken symmetries. It can be expected that whenever the subtraction point is shifted to fine tune the overall position of a multiplet of resonances, any spurious binding will produce at most a residual distortion in the individual positions, without compromising the existence and main couplings of the resonances under study.

III. RESULTS AND DISCUSSION

A. Λ_b and Λ_b^* states

In the Λ_b sector ($B = -1$, $C = 0$, $S = 0$, $I = 0$, $J^P = 1/2^-$), the following sixteen channels are involved:

$$\Sigma_b\pi \;\; \Lambda_b\eta \;\; N\bar{B} \;\; N\bar{B}^* \;\; \Xi_b K \;\; \Lambda_b\omega \;\; \Xi_b'K \;\; \Lambda\bar{B}_s^0$$
$$\Lambda\bar{B}_s^* \;\; \Lambda_b\eta' \;\; \Sigma_b\rho \;\; \Sigma_b^*\rho \;\; \Lambda_b\phi \;\; \Xi_b K^* \;\; \Xi_b'K^* \;\; \Xi_b^*K^*$$

Likewise for the Λ_b^* sector ($B = -1$, $C = 0$, $S = 0$, $I = 0$, $J^P = 3/2^-$), there are eleven channels:

$$\Sigma_b^*\pi \;\; N\bar{B}^* \;\; \Lambda_b\omega \;\; \Xi_b^*K \;\; \Lambda\bar{B}_s^* \;\; \Sigma_b\rho$$
$$\Sigma_b^*\rho \;\; \Lambda_b\phi \;\; \Xi_b K^* \;\; \Xi_b'K^* \;\; \Xi_b^*K^*$$

In both cases the channels are ordered by increasing mass thresholds.

By solving the coupled-channel Bethe-Salpeter equation several states are generated in each of the two sectors. The three lowest lying Λ_b resonances have masses of 5880 and 5949 MeV ($J^P = 1/2^-$) and 5963 MeV ($J^P = 3/2^-$). As one can expect, the situation in the $J = 1/2^-$ channel keeps a close parallelism with that of the $\Lambda_c(2595)$ resonance in the charm sector [46, 47]. For both heavy flavors the structure obtained mimics the well-known two-pole pattern of the $\Lambda(1405)$ [20, 23, 25]. Thus, we find that the state at 5880 strongly couples to

the $N\bar{B}$ and $N\bar{B}^*$ channels, with a negligible $\Sigma_b\pi$ coupling, while the 5949 MeV state has a sizable coupling to this latter channel. On the other hand, the $J^P = 3/2^-$ state at 5963 is generated mainly by the ($N\bar{B}^*$, $\Sigma_b^*\pi$) coupled-channel dynamics. This state is the bottom counterpart of the $\Lambda(1520)$ and $\Lambda_c^*(2625)$ resonances.

These results are encouraging, but to achieve a better description of the $\Lambda_b(5912)$ and $\Lambda_b(5920)$ states reported by the LHCb Collaboration, we have slightly changed the value of the subtraction point used in the RS defined by Eqs. (3) and (4) [46]. Thus, in this sector, we have set the meson-baryon loop to be zero at the C.M. energy $\sqrt{s} = \mu$ given by

$$\mu^2 = \alpha \left(M_{\Sigma_b}^2 + m_\pi^2 \right) . \tag{6}$$

For $\alpha = 0.967$, we find two poles above the $\Lambda_b^0\pi\pi$ threshold, with masses 5910.1 MeV ($J^P = 1/2^-$) and 5921.5 MeV ($J^P = 3/2^-$), which admit a natural identification with the two experimental Λ_b resonances observed in [1]. The results for masses, widths and couplings are presented in the Table III. We have assigned well-defined group labels to the resonances. The multiplets of SU(6) × HQSS and of SU(3) × HQSS to which the resonances belong are identified by means of the procedure discussed at length in Ref. [47], namely, by adiabatically following the trajectories of the poles generated as the various symmetries are restored or broken. The mass differences ΔM_R of the resonances with respect of ground state Λ_b are also shown in Table III.

$$\Delta M_R = M_R - M_{\Lambda_b(g.s.)} \tag{7}$$

For each resonance, the decay mode with largest phase-space allowed by strong interactions (or electromagnetic ones when the strong decay is forbidden) is shown in the last column.

We find that the states $\Lambda_b(5912)$ and $\Lambda_b^*(5920)$ are heavy-quark spin symmetry partners. Indeed, these two states would be part of a 3^* irreducible representation (irrep) of SU(3), embedded in a **15** irrep of SU(6) (which in turn belongs to the irrep **168** of SU(8) [47]). Thus, the light quark structure of these two states is the same, and in particular their total spin, $s_l = 1$. Hence, the coupling of the b-quark spin ($j_b = 1/2$) with the spin of the light degrees of freedom yields $J = 1/2$ and $J = 3/2$. Then the two states, $\Lambda_b(5912)$ and $\Lambda_b^*(5920)$, form an approximate degenerate doublet; they are connected by a spin rotation of the b-quark.

Comparison of Table III with the Table III of Ref. [47] in the charm sector, shows that states with the same group labels in both tables are the heavy flavor counterpart of each other. In particular, the $\Lambda_b(5920)$ resonance is the bottom version of $\Lambda_c(2625)$ one, while the $\Lambda_b(5912)$ would not be the counterpart of the $\Lambda_c(2595)$ resonance, but it would be of the second charmed state that appears around 2595 MeV, and that gives rise to the two pole structure [47] mentioned above. The same conclusion follows from inspection of their couplings: the $\Lambda_c(2595)$ couples weakly to $\Sigma_c\pi$ while the coupling to $\Sigma_b\pi$ is sizable for the $\Lambda_b(5912)$ state.

---

[5] Simultaneously, we find that the gaps between resonances decrease as $1/m_Q$.

SU(6) irrep	SU(3)$_{2J+1}$ irrep	ΔM_R MeV	M_R MeV	Γ_R	Couplings to main channels	J	Experimental LHCb	Decay mode
21	**3$^*_2$**	178	5797.6	0	$g_{N\bar B}=4.9$, $g_{N\bar B^*}=8.3$, $g_{\Lambda\bar B_s^0}=2.1$, $g_{\Lambda\bar B_s^*}=3.6$, $g_{\Lambda_b\eta'}=1.0$, $g_{\Sigma_b^*\rho}=0.6$	1/2		$\Lambda_b\gamma$
15	**3$^*_2$**	291	5910.1	0	$g_{\Sigma_b\pi}=1.8$, $g_{N\bar B}=4.6$, $g_{N\bar B^*}=3.0$, $g_{\Lambda_b\omega}=1.4$	1/2	$\Lambda_b(5912)$	$\Lambda_b\pi\pi$
15	**3$^*_4$**	301	5921.5	0	$g_{\Sigma_b^*\pi}=1.8$, $g_{N\bar B^*}=5.7$, $g_{\Lambda_b\omega}=1.5$	3/2	$\Lambda_b^*(5920)$	$\Lambda_b\pi\pi$
21	**3$^*_2$**	390	6009.3	0	$\mathbf{g_{\Sigma_b\pi} \sim 0.05}$, $g_{\Lambda_b\eta}=2.0$, $g_{N\bar B}=1.1$, $g_{N\bar B^*}=1.7$, $g_{\Xi_b K}=0.8$, $g_{\Lambda\bar B_s^*}=3.9$, $g_{\Sigma_b^*\rho}=0.7$, $g_{\Xi_b^* K^*}=0.9$	1/2		$\Sigma_b\pi$

TABLE III: Λ_b ($J^P = 1/2^-$) and Λ_b^* ($J^P = 3/2^-$) resonances predicted in this work. The parameter α in Eq. (6) has been set to 0.967. The SU(6) and SU(3) × SU(2) representations of the corresponding states are shown in the first two columns. M_R, Γ_R and ΔM_R stand for the mass, the width, and the mass difference with respect to the ground state ($J^P = 1/2^+$) Λ_b. The next column displays the (absolute value of the) dominant couplings to the different meson-baryon channels, ordered by their threshold energies. The couplings to channels open for decay are highlighted in bold font. The seventh column shows the spin of the resonance. Tentative identifications with experimental resonances of LHCb are also given in the following column. Finally, in the last column we show the decay channel with largest phase-space allowed by strong interactions (or electromagnetic ones when the strong decay is forbidden). The two states in the **15** of SU(6) form a HQSS doublet, the other two states are HQSS singlets. The three lightest states belong to the **168** of SU(8), the heaviest one belongs to the **120** (note that it is precisely in these two SU(8) irreps where the WT interaction is more attractive, and thus the lowest-lying states stem from them [47]).

The two states observed by the LHCb Collaboration are detected through their decay to Λ_b(g.s.)$\pi\pi$. The fit to the data of the experiment of Ref. [1] yields

$$N(pp \to \Lambda_b^*(5920) \to \Lambda_b\pi\pi) = 16.4 \pm 4.7 \qquad (8)$$

events with mass $M_{\Lambda_b(5912)} = 5911.95 \pm 0.11\,\text{MeV}$ and

$$N(pp \to \Lambda_b(5912) \to \Lambda_b\pi\pi) = 49.5 \pm 7.9 \qquad (9)$$

events with mass $M_{\Lambda_b^*(5920)} = 5919.76 \pm 0.07\,\text{MeV}$. The experimental setup of LHCb and the strong decay mechanism of the resonances observed, guarantees that the decay to $\Lambda_b\pi\pi$ always takes place within the space and time intervals set for detection [68]. Therefore no bias is expected from the possible different decay rates of the two resonances, and

$$\frac{N(pp \to \Lambda_b^*(5920))}{N(pp \to \Lambda_b(5912))} = \frac{N(pp \to \Lambda_b^*(5920) \to \Lambda_b\pi\pi)}{N(pp \to \Lambda_b(5912) \to \Lambda_b\pi\pi)}. \qquad (10)$$

This translates into an experimental ratio of cross sections

$$\left.\frac{\sigma(pp \to \Lambda_b^*(5920))}{\sigma(pp \to \Lambda_b(5912))}\right|_{\text{exp}} = \frac{N(pp \to \Lambda_b^*(5920))}{N(pp \to \Lambda_b(5912))} = 3.0 \pm 1.0 \qquad (11)$$

From the theoretical side, due to the dominant strong interactions taking place during creation and hadronization of the quark b, a natural assumption is that the b-quark spin ends up in a random state. In that case, and assuming that $\Lambda_b(5912)$ and $\Lambda_b^*(5920)$ form a HQSS doublet, the ratio of production of these states should be the quotient of multiplicities, that is:

$$\frac{\sigma(pp \to \Lambda_b^*(5920))}{\sigma(pp \to \Lambda_b(5912))} \approx \frac{2J_{\Lambda_b^*}+1}{2J_{\Lambda_b}+1} = 2. \qquad (12)$$

Although not fully satisfactory, this ratio is not inconsistent with the observed ratio, in Eq. (11), and it gives support to our conclusion that the two observed states form a HQSS doublet.

From the couplings shown in Table III, the dominant decay mechanism of $\Lambda_b(5912)$ is expected to be of the form $\Lambda_b(5912) \to \Sigma_b\pi$ with subsequent decay of the off-shell heavy baryon, $\Sigma_b \to \Lambda_b\pi$. Its heavy quark partner follows a similar pattern with Σ_b^* and Λ_b^*. The approximate HQSS requires the two resonances to have a similar width. In order to estimate this width, we consider the following effective Lagrangian

$$\mathcal{L}(x) = \frac{g_{\Sigma_b\pi}}{\sqrt{3}} \vec{\Sigma}_b^\dagger \vec\pi \Lambda_b^{\text{res}} + g\, \vec{\Sigma}_b^\dagger \sigma_i \partial_i \vec\pi\, \Lambda_b + \text{h.c.} \qquad (13)$$

The averaged experimental decay width of the Σ_b, 7.3 MeV, allows to extract the value $g \approx 51$. The value of $g_{\Sigma_b\pi} = 1.8$ taken from our calculation, Table III, gives a small width for $\Lambda_b(5912)$ around 8 keV. A similar calculation for $\Lambda_b^*(5920)$ yields a width around 12 keV.[6] The smallness of the widths are due to the reduced phase space available since the resonances are fairly close to the threshold. This is consistent with the experimental bounds quoted in [1].

Different quark models [2, 4–7] have also conjectured the existence of one or more excited $\Lambda_b(1/2^-)$ and $\Lambda_b(3/2^-)$ states. While the predicted masses for [4–7] differ few tenths of MeV from the LHCb experimental ones (see Table VIII of Ref. [7] for a summary of some

---

[6] These numbers are just estimates. Being close to threshold any refinement in the treatment will induce relatively large changes in the values quoted.

of the results), the early work of Capstick and Isgur [2] generated the first two excited $\Lambda_b(1/2^-)$ and $\Lambda_b(3/2^-)$ states with masses that are in very good agreement with the ones observed by the LHCb collaboration. However, the ground state $\Lambda_b(1/2^+)$ mass in this scheme is below the experimental one. Our model reproduces the experimental $\Lambda_b(5912)$ and $\Lambda_b(5920)$ but with an alternative explanation of their nature as molecular states, which moreover are HQSS partners.

B. Ξ_b and Ξ_b^* states

Next, we analyze the ($B = -1$, $C = 0$, $S = -1$, $I = 1/2$) sector, for both $J = 1/2$ and $J = 3/2$ spins (Ξ_b and Ξ_b^* states, respectively). Our model predicts the existence of nine states (6 Ξ_b and 3 Ξ_b^*) stemming from the strongly attractive **120** and **168** SU(8) irreducible representations (see Ref. [47] for the analogous charm sector). However, only three Ξ_b and one Ξ_b^* belong to the same SU(3)×HQSS multiplets of the Λ_b and Λ_b^* states reported in Table III. In this exploratory study, we restrict our discussion only to these states.

In the Ξ_b sector, the following thirty one channels are involved:

$$\Xi_b\pi \quad \Xi_b'\pi \quad \Lambda_b\bar{K} \quad \Sigma_b\bar{K} \quad \Xi_b\eta \quad \Lambda\bar{B} \quad \Lambda\bar{B}^* \quad \Sigma\bar{B}$$
$$\Xi_b'\eta \quad \Lambda_b\bar{K}^* \quad \Sigma\bar{B}^* \quad \Omega_bK \quad \Xi_b\rho \quad \Xi_b\omega \quad \Xi\bar{B}_s \quad \Xi_b'\rho$$
$$\Sigma_b\bar{K}^* \quad \Xi_b'\omega \quad \Sigma^*\bar{B}^* \quad \Xi_b^*\rho \quad \Sigma_b^*\bar{K}^* \quad \Xi_b^*\omega \quad \Xi\bar{B}_s^* \quad \Xi_b\eta'$$
$$\Xi_b\phi \quad \Xi_b'\eta' \quad \Omega_bK^* \quad \Xi_b'\phi \quad \Xi^*\bar{B}_s^* \quad \Omega_b^*K^* \quad \Xi_b^*\phi$$

while in the Ξ_b^* sector, the twenty six channels, ordered by increasing thresholds, are:

$$\Xi_b^*\pi \quad \Sigma_b^*\bar{K} \quad \Lambda\bar{B}^* \quad \Xi_b^*\eta \quad \Lambda_b\bar{K}^* \quad \Sigma\bar{B}^* \quad \Omega_b^*K \quad \Xi_b\rho$$
$$\Xi_b\omega \quad \Sigma^*\bar{B} \quad \Xi_b'\rho \quad \Sigma_b\bar{K}^* \quad \Xi_b'\omega \quad \Sigma^*\bar{B}^* \quad \Xi_b^*\rho \quad \Sigma_b^*\bar{K}^*$$
$$\Xi_b^*\omega \quad \Xi\bar{B}_s^* \quad \Xi_b\phi \quad \Xi^*\bar{B}_s \quad \Xi_b'\eta' \quad \Omega_bK^* \quad \Xi_b'\phi \quad \Xi^*\bar{B}_s^*$$
$$\Omega_b^*K^* \quad \Xi_b^*\phi$$

For the subtraction point we use $\mu^2 = M_{\Xi_b}^2 + m_\pi^2$, and thus we assume our default value $\alpha = 1$ in Eq. (6). There is no particularly good reason to use the same value as in the Λ_b case. Even SU(3) does not relate the two μ^{SI} points, $M_{\Sigma_b}^2 + m_\pi^2$ and $M_{\Xi_b}^2 + m_\pi^2$, required to fix the RS in each sector. If instead we take $\alpha = 0.967$ as in the Λ_b sector, Ξ_b and Ξ_b^* binding energies (masses) will be larger (smaller) by about 60-80 MeV. These 60-80 MeV should be admitted as an intrinsic systematic uncertainty in our predictions in this sector.

In this way, we find the Ξ_b and Ξ_b^* states that complete the Λ_b and Λ_b^* SU(3)×HQSS multiplets. The properties of the dynamically generated Ξ_b and Ξ_b^* states are compiled in Table IV. By studying the evolution of the poles from the SU(6)×HQSS symmetric point, we find that $\Lambda_b(5797.6)$ and $\Xi_b(5874)$ belong to the same irreducible representation, and similarly the $\Lambda_b(6009.3)$ and $\Xi_b(6072.8)$ states. Also, the pair $\Xi_b(6035.4)$ and $\Xi_b^*(6043.3)$, in the **15** irrep of SU(6),

form the HQSS doublet related by SU(3) to the doublet formed by the $\Lambda_b(5910.1)$ and $\Lambda_b^*(5921.5)$ states.

The three Ξ_b and one Ξ_b^* states have also partners in the charm sector. We find that states with the same group labels are the heavy flavor counterpart of each other, as already noted for the Λ_b and Λ_b^* sectors. By comparing Table IV with Table V of Ref. [47], we see that the HQSS partners in the charm sector coming from the **15** representation, $\Xi_c(2772.9)$ and $\Xi_c^*(2819.7)$, are the bottom counterparts of the $\Xi_b(6035.4)$ and $\Xi_b^*(6043.3)$ states. Moreover, the charmed $\Xi_c(2699.4)$ and $\Xi_c(2775.4)$ resonances are analogous to the $\Xi_b(5874)$ and $\Xi_b(6072.8)$ ones in the bottom sector, respectively. None of these bottomed states have been seen experimentally yet. Schemes based on quark models [2, 4–7] predict $\Xi_b(1/2^-)$ and $\Xi_b(3/2^-)$ states with similar masses to our estimates, though there exist some differences between the various predictions. The experimental observation of the Ξ_b and Ξ_b^* excited states and their decays might, on the other hand, provide some valuable information concerning the nature of these states, whether they can be described as pure quark states or they have an important molecular component.

Fig. 1 shows a summary of the masses of the predicted $\Lambda_b(1/2^-)$, $\Lambda_b(3/2^-)$, $\Xi_b(1/2^-)$ and $\Xi_b(3/2^-)$ states with respect to the mass of the ground state Λ_b, together with several thresholds for possible two- and three-body decay channels. The experimental $\Lambda_b^0(5912)$ and $\Lambda_b^0(5920)$ of LHCb are given for reference. Tables III and IV show that, except for $\Xi_b(6072.8)$, our predicted states have a negligible width. This implies that they do not strongly couple to two-body channels with lower mass, such as $\Sigma_b\pi$ or $\Xi_b\pi$. Three-body channels are not included in our calculation. These channels allow the possibility of strong decay for some of the states. This is the case of the $\Lambda_b(3/2^-)$ and the two $\Lambda_b(1/2^-)$ which lie above the threshold of $\Lambda_b\pi\pi$, but it is not the case for the lightest Λ_b and Ξ_b states. They are below all hadronic channels, and hence they are stable under strong interactions. These states could be detected through electric dipole decay to $\Lambda_b\gamma$ and $\Xi_b\gamma$. Note that the strong decay of $\Xi_b(3/2^-)$ to $\Xi_b\pi$ is forbidden in s-wave but allowed through d-wave mechanisms not included in our model.

In Fig. 2, we depict $(\pm|T|)$−matrix for the four (SIJ) sectors studied in this work. Sectors related through SU(3) or by HQSS are plotted with opposite sign to better appreciate the degree of fulfillment or breaking of these symmetries. The extra poles stand for other states which stem from other SU(8)/SU(6) irreps to those considered in this exploratory study.

IV. CONCLUSIONS

We have analyzed odd parity baryons with one bottom quark by means of a unitarized meson-baryon coupled-channel model which implements heavy-quark

SU(6) irrep	SU(3)$_{2J+1}$ irrep	ΔM_R MeV	M_R MeV	Γ_R MeV	Couplings to main channels	J	Main decay mode
21	$\mathbf{3_2^*}$	255	5874.	0.	$g_{\Lambda\bar{B}}=1.3,\ g_{\Sigma\bar{B}}=4.4,\ g_{\Lambda\bar{B}^*}=2.3,\ g_{\Sigma\bar{B}^*}=7.3,$ $g_{\Xi\bar{B}_s}=2.6,\ g_{\Xi_b\eta'}=1.0,\ g_{\Xi\bar{B}_s^*}=4.5$	1/2	$\Xi_b\gamma$
15	$\mathbf{3_2^*}$	416	6035.4	0.	$\mathbf{g_{\Xi_b\pi}\sim 0.05},\ g_{\Sigma_b\bar{K}}=2.3,\ g_{\Lambda\bar{B}}=1.,\ g_{\Sigma\bar{B}}=4.5,$ $g_{\Sigma\bar{B}^*}=2.8,\ g_{\Xi_b\omega}=1.2,\ g_{\Sigma^*\bar{B}^*}=2.3$	1/2	$\Xi_b\pi$
15	$\mathbf{3_4^*}$	424	6043.3	0.	$g_{\Sigma_b^*\bar{K}}=2.3,\ g_{\Lambda\bar{B}^*}=1.1,\ g_{\Sigma\bar{B}^*}=5.5,\ g_{\Sigma^*\bar{B}}=1.4,$ $g_{\Xi_b\omega}=1.2,\ g_{\Sigma^*\bar{B}^*}=1.7$	3/2	$\Xi_b\pi$
21	$\mathbf{3_2^*}$	453	6072.8	0.3	$\mathbf{g_{\Xi_b\pi}=0.1},\ \mathbf{g_{\Xi_b'\pi}=0.1},\ g_{\Xi_b\eta}=2.4,\ g_{\Lambda\bar{B}}=1.4,$ $g_{\Lambda\bar{B}^*}=2.3,\ g_{\Sigma\bar{B}}=1.1,\ g_{\Sigma\bar{B}^*}=1.6,\ g_{\Xi\bar{B}_s}=2.9,$ $g_{\Xi\bar{B}_s^*}=4.5$	1/2	$\Xi_b\pi,\ \Xi_b'\pi$

TABLE IV: SU(3) partners of the states in Table III. Predictions for Ξ_b ($J^P=1/2^-$) and Ξ_b^* ($J^P=3/2^-$) resonances (with $\alpha=1$ in Eq. (6)). No experimental excited Ξ_b or Ξ_b^* resonances have been detected yet. The two states in the **15** of SU(6) form a HQSS doublet.
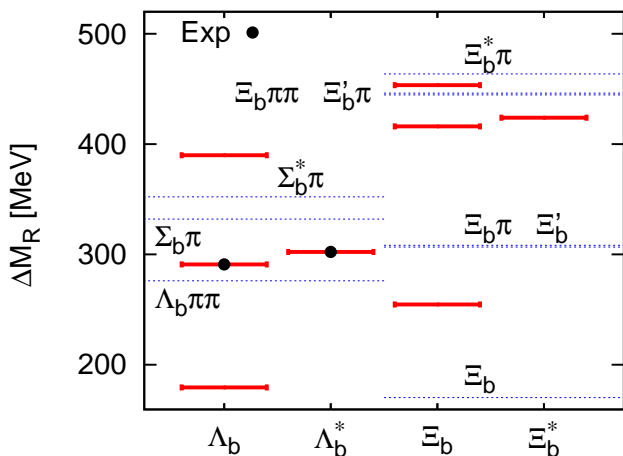

FIG. 1: Summary of the new predicted states. We also show the experimentally observed $\Lambda_b^0(5912)$ and $\Lambda_b^0(5920)$ states and some relevant hadronic thresholds.

FIG. 2: $\pm\max_j\sum_i|T_{ij}(\sqrt{s})|$ for the four (I,J) sectors studied. We use "plus" sign for the sectors Λ_b (blue, solid line) and Ξ_b^* (red, dashed line) and "minus" sign for Λ_b^* (blue, solid line) and Ξ_b (red, dashed line). Exact SU(3) or HQSS symmetries would translate into exact mirror symmetries in the plot.

spin symmetry. In particular, pseudoscalar and vector heavy mesons are treated on an equal footing. We rely on a relatively simple tree-level contact interaction already used in the charm sector [46, 47]: the matrix elements follow from Clebsch-Gordan coefficients of the underlying spin-flavor symmetry with no free-parameters. This interaction has the virtue of embodying the approximate patterns of chiral symmetry, when Goldstone bosons are involved, and HQSS when heavy hadrons are present.

A summary of our predictions is graphically shown in Fig. 1. The experimental states $\Lambda_b^0(5912)$ and $\Lambda_b^0(5920)$ reported by the LHCb collaboration are obtained as dynamically generated meson-baryon molecular states. Within our scheme, these states are identified as HQSS partners, which naturally explain their approximate mass degeneracy. Other $\Lambda(1/2^-)$ states coming from the same attractive SU(6) × HQSS representations are
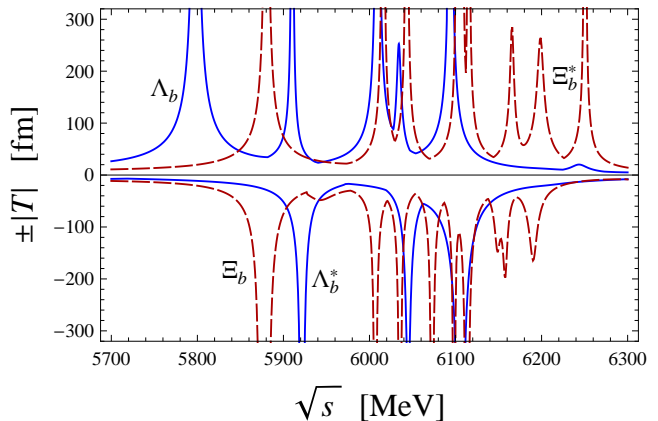
also analyzed and we find a close analogy to the charm and strange sectors. In particular, the $\Lambda_b^0(5920)$ is the bottomed counterpart of the $\Lambda^*(1520)$ and $\Lambda_c^*(2625)$ resonances. Moreover, the $\Lambda_b^0(5912)$ is part of a two-pole structure similar as the one observed in the case of the $\Lambda(1405)$ and $\Lambda_c(2595)$ resonances.

Mass and decay mode predictions are also obtained for some $\Xi_b(1/2^-)$ and $\Xi_b(3/2^-)$ resonances, which belong to the same SU(3) multiplets as the $\Lambda_b(1/2^-)$ and $\Lambda_b(3/2^-)$ states. We find three $\Xi_b(1/2^-)$ and one $\Xi_b(3/2^-)$ states coming from the most attractive SU(6) × HQSS representations. Two of these predicted states, $\Xi_b(6035.4)$ and $\Xi_b^*(6043.3)$, form a HQSS doublet similar to that formed by the experimental $\Lambda_b(5912)$ and $\Lambda_b^*(5920)$ resonances. None of these states have been detected yet, and their existence is also predicted by constituent quark models. It constitutes a clear case for discovery.

[1] R. Aaij *et al.* [LHCb Collaboration], Phys. Rev. Lett. **109** (2012) 172003.

[2] S. Capstick and N. Isgur, Phys. Rev. D **34** (1986) 2809.

[3] J. Beringer *et al.* [Particle Data Group Collaboration], Phys. Rev. D **86** (2012) 010001.

[4] H. Garcilazo, J. Vijande and A. Valcarce, J. Phys. G **34** (2007) 961

[5] D. Ebert, R. N. Faustov and V. O. Galkin, Phys. Lett. B **659** (2008) 612

[6] M. Karliner, B. Keren-Zur, H. J. Lipkin and J. L. Rosner, Annals Phys. **324** (2009) 2

[7] W. Roberts and M. Pervin, Int. J. Mod. Phys. A **23** (2008) 2817

[8] P. G. Ortega, D. R. Entem and F. Fernandez, arXiv:1210.2633 [hep-ph].

[9] E. Klempt and J. -M. Richard, Rev. Mod. Phys. **82**, 1095 (2010)

[10] N. Kaiser, P. B. Siegel and W. Weise, Nucl. Phys. A **594** (1995) 325 [nucl-th/9505043].

[11] N. Kaiser, P. B. Siegel and W. Weise, Phys. Lett. B **362**, 23 (1995).

[12] E. Oset and A. Ramos, Nucl. Phys. A **635**, 99 (1998).

[13] B. Krippa, Phys. Rev. C **58** (1998) 1333; B. Krippa and J. T. Londergan, Phys. Rev. C **58** (1998) 1634.

[14] J. C. Nacher, A. Parreno, E. Oset, A. Ramos, A. Hosaka and M. Oka, Nucl. Phys. A **678**, 187 (2000).

[15] U. G. Meissner and J. A. Oller, Nucl. Phys. A **673**, 311 (2000).

[16] J. A. Oller and U. G. Meissner, Phys. Lett. B **500**, 263 (2001).

[17] J. Nieves and E. Ruiz Arriola, Phys. Rev. D **64**, 116008 (2001).

[18] T. Inoue, E. Oset and M. J. Vicente Vacas, Phys. Rev. C **65**, 035204 (2002).

[19] M. F. M. Lutz and E. E. Kolomeitsev, Nucl. Phys. A **700** (2002) 193

[20] C. Garcia-Recio, J. Nieves, E. Ruiz Arriola and M. J. Vicente Vacas, Phys. Rev. D **67**, 076009 (2003).

[21] E. Oset, A. Ramos and C. Bennhold, Phys. Lett. B **527** (2002) 99 [Erratum-ibid. B **530** (2002) 260] [nucl-th/0109006].

[22] A. Ramos, E. Oset and C. Bennhold, Phys. Rev. Lett. **89**, 252001 (2002).

[23] D. Jido, J. A. Oller, E. Oset, A. Ramos and U. G. Meissner, Nucl. Phys. A **725**, 181 (2003).

[24] L. Tolos, A. Ramos, A. Polls and T. T. S. Kuo, Nucl. Phys. A **690**, 547 (2001).

[25] C. Garcia-Recio, M. F. M. Lutz and J. Nieves, Phys. Lett. B **582** (2004) 49

[26] J. A. Oller, J. Prades and M. Verbeni, Phys. Rev. Lett. **95**, 172502 (2005).

[27] B. Borasoy, R. Nissler and W. Weise, Eur. Phys. J. A **25**, 79 (2005).

[28] B. Borasoy, U. G. Meissner and R. Nissler, Phys. Rev. C **74**, 055201 (2006).

[29] T. Hyodo, D. Jido and A. Hosaka, Phys. Rev. C **78**, 025203 (2008).

[30] L. Tolos, J. Schaffner-Bielich and A. Mishra, Phys. Rev. C **70**, 025203 (2004).

[31] M. F. M. Lutz and E. E. Kolomeitsev, Nucl. Phys. A **730**, 110 (2004).

[32] M. F. M. Lutz and E. E. Kolomeitsev, Nucl. Phys. A **755**, 29 (2005)

[33] J. Hofmann and M. F. M. Lutz, Nucl. Phys. A **763**, 90 (2005)

[34] J. Hofmann and M. F. M. Lutz, Nucl. Phys. A **776**, 17 (2006).

[35] M. F. M. Lutz and C. L. Korpa, Phys. Lett. B **633** (2006) 43 [nucl-th/0510006].

[36] T. Mizutani and A. Ramos, Phys. Rev. C **74**, 065201 (2006)

[37] L. Tolos, A. Ramos and T. Mizutani, Phys. Rev. C **77**, 015207 (2008).

[38] C. E. Jimenez-Tejero, A. Ramos and I. Vidana, Phys. Rev. C **80**, 055206 (2009)

[39] J. Haidenbauer, G. Krein, U. G. Meissner and A. Sibirtsev, Eur. Phys. J. A **33**, 107 (2007).

[40] J. Haidenbauer, G. Krein, U. G. Meissner and A. Sibirtsev, Eur. Phys. J. A **37**, 55 (2008).

[41] J. Haidenbauer, G. Krein, U. G. Meissner and L. Tolos, Eur. Phys. J A **47**, 18 (2011)

[42] J. -J. Wu, R. Molina, E. Oset and B. S. Zou, Phys. Rev. Lett. **105**, 232001 (2010);

[43] J. -J. Wu, R. Molina, E. Oset and B. S. Zou, Phys. Rev. C **84** (2011) 015202

[44] E. Oset, A. Ramos, E. J. Garzon, R. Molina, L. Tolos, C. W. Xiao, J. J. Wu and B. S. Zou, Int. J. Mod. Phys. E **21** (2012) 1230011.

[45] J. -J. Wu and B. S. Zou, Phys. Lett. B **709** (2012) 70.

[46] C. Garcia-Recio, V. K. Magas, T. Mizutani, J. Nieves, A. Ramos, L. L. Salcedo and L. Tolos, Phys. Rev. D **79**, 054004 (2009)

[47] O. Romanets, L. Tolos, C. Garcia-Recio, J. Nieves, L. L. Salcedo and R. G. E. Timmermans, Phys. Rev. D **85** (2012) 114032.

[48] D. Gamermann, C. Garcia-Recio, J. Nieves, L. L. Salcedo and L. Tolos, Phys. Rev. D **81** (2010) 094016

[49] N. Isgur and M. B. Wise, Phys. Lett. B **232** (1989) 113.

[50] M. Neubert, Phys. Rep. **245** 259 (1994).

[51] A.V. Manohar and M.B. Wise, *Heavy Quark Physics*, Cambridge Monographs on Particle Physics, Nuclear Physics and Cosmology, vol. 10

[52] D. Gamermann, C. Garcia-Recio, J. Nieves and L. L. Salcedo, Phys. Rev. D **84** (2011) 056017.

[53] C. Garcia-Recio, J. Nieves, L. L. Salcedo and L. Tolos, Phys. Rev. C **85** (2012) 025203.

[54] E. Oset, private communication.

[55] C. Garcia-Recio, J. Nieves and L. L. Salcedo, Phys. Rev. D **74** (2006) 034025 [hep-ph/0505233].

[56] Combination of the world average [3] and the LHCb measurement [57] employed in [1] for analyzing the $\Lambda_b^0 \pi^+ \pi^-$ spectrum.

[57] R. Aaij *et al.* [LHCb Collaboration], Phys. Lett. B **708** (2012) 241.

[58] Average of [59] (lattice), [60] (quark model), [61] (QCD sum rules), and [62] ($1/N_c$ expansion).

[59] K. C. Bowler *et al.* [UKQCD Collaboration], Phys. Rev. D **54** (1996) 3619.

[60] C. Albertus, J. E. Amaro, E. Hernandez and J. Nieves, Nucl. Phys. A **740** (2004) 333.

[61] Z. -G. Wang, Phys. Lett. B **685** (2010) 59.

[62] E. E. Jenkins, Phys. Rev. D **77** (2008) 034012.

[63] S. Chatrchyan *et al.* [CMS Collaboration], Phys. Rev. Lett. **108** (2012) 252002

[64] LHCb Collaboration, "Measurement of the masses of the Ξ_b^- and Ω_b^-", LHCb-CONF-2011-060, CERN-LHCb-CONF-2011-060, http://cdsweb.cern.ch/record/1395530/files/LHCb-CONF-2011-060.pdf

[65] A. Ali Khan, T. Bhattacharya, S. Collins, C. T. H. Davies, R. Gupta, C. Morningstar, J. Shigemitsu and J. H. Sloan, Phys. Rev. D **62** (2000) 054505.

[66] H. Na, C. J. Monahan, C. T. H. Davies, R. Horgan, G. P. Lepage and J. Shigemitsu, arXiv:1202.4914 [hep-lat].

[67] C. McNeile, C. T. H. Davies, E. Follana, K. Hornbostel and G. P. Lepage, Phys. Rev. D **85** (2012) 031503

[68] A. Poluektov (LHCb Collaboration), private communication.